



Flexural strength prediction of randomly oriented chopped glass fiber composite laminate using artificial neural network

Pankaj Chaupal¹ · Prakash Rajendran¹

Received: 22 October 2022 / Accepted: 24 January 2023 / Published online: 6 February 2023
© The Author(s), under exclusive licence to The Brazilian Society of Mechanical Sciences and Engineering 2023

Abstract

Randomly oriented chopped glass fiber reinforced polymer (ROCGFRP) composite laminate exhibits better flexural behavior, intended to use in various industrial applications such as aerospace, automobile, defence and marine engineering industries. This work employs the artificial neural network (ANN) model to predict the flexural strength of the randomly oriented chopped glass fiber composite beam using MATLAB[®]2021a. For this purpose, experimental flexural strength test based on ASTM D790 and finite element analysis (FEA) simulation with cohesive zone model using ANSYS Workbench 19.2 were conducted to compute the input and output parameters for the ANN model. Strain and stress datasets were chosen as the model's input and output parameters, respectively. The entire datasets i.e., seven thousand six hundred and sixteen points, were divided into training, validation and test sets in the proportion of 70:15:15, respectively. The appropriate structure of the ANN model such as input layer, hidden layer, output layer, activation functions and training algorithm are selected and evaluated using statistical tools. The number of neurons in the hidden layer is optimized using Levenberg-Marquardt training algorithm. The training, validation and test components are fitted along the regression line, which shows strong relationship between analysis and desired outcomes. Thus, it is observed that, there is a high level of consistency is observed among the numerical, experimental and predicted results. Finally, the obtained ANN model is good predictor for flexural strength of ROCGFRP composite laminate.

Keywords Randomly oriented chopped glass fiber · Flexural strength · Three-point bending test · Finite element method · Cohesive zone method · Artificial neural network

List of Abbreviations

ANN	Artificial neural network	RBFNN	Radial basis function neural network
BP	Back-propagation	RMS	Root mean square
CZM	Cohesive zone method	ROCGFRP	Randomly oriented chopped glass fiber reinforced polymer
FE	Finite element	SVM	Support vector machine
FEA	Finite element analysis	UTM	Universal testing machine
GFRP	Glass fiber reinforced polymer	VLRBP	Variable learning rate back propagation
GRNN	Generalised regression neural network		
L–M	Levenberg–Marquardt		
PVA	Poly-vinyl alcohol		
PLA	Polylactic acid		
QN	Quasi Newton		
RBP	Resilient back propagation		

Technical Editor: João Marciano Laredo dos Reis.

✉ Prakash Rajendran
rprakash@nitt.edu

¹ Department of Mechanical Engineering, National Institute of Technology, Tiruchirappalli 620015, Tamil Nadu, India

1 Introduction

Composite materials are formed of atleast two materials, namely fiber-reinforced and matrix without blending, that work together to offer substantial material properties that differ from the properties of individual components. [1–3]. Glass fibre reinforced polymer (GFRP) composite laminates are mostly utilized in structures that require high specific strength and stiffness, as well as resistance to fatigue and corrosion. It enables the development of lighter structures and it's applications are seen in the aerospace, automotive,

defence, infrastructure, maritime, sports, oil and gas industries [4–7]. GFRP composite laminates accounts for more than 95 percentage of maritime applications due to its economic advantage over the carbon fibre composites [8]. Fiber-reinforced mats are available in a variety of fibre orientations, including randomly oriented, uni-directional, and bi-directional forms. It gives the considerable strength to composite. Further, the job of matrix is to bind the fibre and accessible in the form of resin. There are two varieties of polyester resins are available in the market. The first type is orthophthallic polyester resin, often known as standard economical polyester resin. It is used in a variety of industrial applications, including wind turbine blades, rotor components, water tanks, sewer pipes, structures, and infrastructure. Other type is isophthalic polyester resin, which is commonly used in the maritime industry because to its great water resistance [9]. The three-point bending test is simple, reliable and sensitive method to compute the load bearing strength of GFRP composite materials [10, 11]. While the laminate is subjected to transverse loads, flexural strength is very remarkable parameter in the design of randomly oriented chopped GFRP composite laminates [12]. Due to the applied transverse loads, the outermost and innermost layers of the laminates are subjected to tensile and compressive stresses respectively. In addition to that, the laminates are also subjected to shear stresses, which is maximum at the neutral axis and becomes zero at the outermost surface [13].

Chaudhary et al. [14] computed the flexural strength of unidirectional GFRP composite laminate experimentally using three point bending test and numerically done by FEA software ANSYS. They found that experimental results holds good with numerical results. Ratnakar and Shivanan [15] performed a three-point bending test for glass/epoxy and graphite fiber-reinforced composites according to ASTM D790 standards and computed flexural strength and stiffness for both specimens. It is observed that graphite-fiber reinforced composite has greater strength and stiffness than glass/epoxy composite. Galbano et al. [16] conducted a three-point bending test on a manufactured composite laminate composed of eight stacking sequences of different fibres including carbon fibre, quartz fibre and glass fibre. It is inferred that flexural strength of carbon and quartz fiber exceeds glass fiber. Wazery et al. [17] fabricated E-glass fiber with random oriented reinforced polymer composite using hand lay-up techniques with varying fiber percentages. They examined that with increase in fiber percentage of mechanical properties such as tensile strength, bending strength, impact strength and hardness increased. Hybridization can enhance the mechanical properties of composite laminates considerably [18]. Dong [19] found that hybridization of symmetric carbon and glass fiber composite laminate can improve the flexural strength. It is also suggested that carbon/epoxy plies should be placed corresponding to the

outer layer of composite to maintain its stiffness. According to Jiang et al. [20] the effect of temperature and moisture leads to degradation of flexural strength of GFRP composite laminates, on both strength and stiffness wise. Damage in the composite laminates may initiate with matrix cracking that leads to delamination. Delamination frequently happens at stress-free edges due to property mismatches at ply interfaces. Cheg et al. [21] developed the finite element (FE) model to investigate the delamination behaviour of composite laminate based on cohesive zone method. The accuracy of FEA vary considerably with mesh size and boundary conditions. Thus experimental and FEA can be combined with machine learning based method to improve effectiveness, efficiency and reliability.

Machine learning based methods are fast, efficient and accurate. It can be used for solving complex non-linear problems. It is inspired by the functionality of human brains and employs billions of interconnected neurons to process data in parallel [22–24]. Support vector machine (SVM) can be used to solve both classification and regression problem [25]. Tanyildizi [26] used ANN and SVM to predict the compressive and flexural strengths of light weight concrete made of silica fume and carbon fiber at varying temperature. It is observed that prediction accuracy and reliability of ANN is better than SVM. Jiang et al. [23] employed the back propagation ANN model to predict tensile, impact, bending strength and wear properties of short fibre reinforced polyamide composite. Zhang and Friedrich [27] reviewed various principle of ANN to estimate fatigue life, wear performance and dynamic properties of polymer composite laminate. Mentges et al. [28] computed micro-mechanical data using FEA and orientation averaging and fed to ANN as input and predicted stiffness of short fiber reinforced composite. ANN model was utilized by Hassan et al. [29] to estimate the fatigue life of glass fiber composite shaft. Gayatri et al. [30] forecasted the tensile strength of hybrid polymer composites using ANN model. Stephen et al. [31] predicted the impact resistance of hybrid and non-hybrid FRP composite plate based on FE simulation results. Chopra et al. [32] noticed that the ANN model works well using Levenberg-Marquardt (L-M) algorithm and sigmoid activation function for predicting tensile and compressive strengths. Koklar et al. [33] examined that L-M algorithm outperforms Resilient Back Propagation (RBP), Quasi Newton (QN) and Variable Learning Rate Back Propagation (VLRBP) algorithms. Most common activation functions used in ANN model's are tan-sigmoid, log-sigmoid and purelin. Generally, tan-sigmoid and log-sigmoid are used in hidden layer and purelin in the output layer [34]. Pazhamannil et al. [35] computed the tensile strength of polylactic acid (PLA) using ANN under varying process parameters such as nozzle temperature, layer thickness, and infill speed. Kumar et al. [36] applied radial basis function neural network (RBFNN) and

generalized regression neural network (GRNN) models on acoustic emission parameters to predict the flexural strength of GFRP composite laminate. They observed that the GRNN model outperforms the RBFNN model. Many researchers also estimated the thermal properties such as heat transfer coefficient, thermal conductivity and viscosity apart from the mechanical properties such as tensile, bending and impact strength using ANN model [37, 38]. They found that ANN is good predictor of thermal properties because of its fault tolerant characteristics and ability to learn and model non-linear and complex relationship.

From the literature survey, it is summarized that several research works have been carried out to predict the mechanical and dynamic characteristics of composite laminates made of continuous unidirectional fibers under different materials and orientations based on various process parameters and micro-mechanical approach employed by ANN model. However, there is no study to predict the flexural strength of ROCGFRP composite laminate using ANN model based on FEA and experimental three-point bending test data. Thus, the novelty of this work to use the numerical simulation with cohesive zone method (CZM) dataset and experimental three-point bending test dataset in the ANN model to compute the flexural strength of ROCGFRP composite laminate. This research article is arranged as follows: The review of ANN model are described in section 2. Methodology includes numerical simulation, materials fabrication and experimental details are explained in section 3. The results and discussions are briefly presented in section 4, and finally, concluding marks are discussed in section 5.

2 Review of artificial neural network

A model based on the working mechanism of biological neurons was developed by Frank Rosenblatt in 1958 and named as “Perceptron”. It was a computer program that used linear mathematical methods [39]. Later, between 1959 and 1980, more improvements to the perceptron were made,

eventually leading to the ANNs. Applications of ANNs can be seen in both industrial and research fields such as pattern recognition, stock market prediction, voice recognition, video games, industrial temperature, force prediction, heat conduction and structural health monitoring, etc. [40–43]. The most significant benefits of adopting ANNs are that they are versatile, which means that they can learn through both supervised and unsupervised algorithms and perform universal evaluations [44]. ANN works on the principle of a biological neuron. It uses past data samples to understand and predict the unknown outcomes in future datasets based on past learning. It consists of several artificial neurons, and a single artificial neuron is called the basic building unit of ANN. It is also referred to as a node. It is made up of inputs, net function, transfer function, and outputs, as shown in Fig. 1. The associated synaptic weights are multiplied by the node’s inputs. Synaptic weights are random numbers that dictate the strength or amplitude of individual inputs to neurons. The single artificial neurons can learn through accomplishing the adjustment of the weights.

Single artificial neurons are not efficient for solving complex tasks and robust computation. Thus, multi layer perceptron (ANN) is created to address the common complex problems such as function approximation, pattern recognition, memory association, and so on. Figure 2 depicts that the ANN system, that composed of three layers: input, hidden and output layers. The implementation stages of the ANN system composed of parameter selection, training and testing. Parameters selection consist of input and output parameters, the number of neurons in the hidden layer, activation functions and the training algorithm. The most widely used activation functions are sigmoid, tanh, gaussian, linear, and threshold [45]. After parameters selection, the networks are fed with sample datasets for training. The training involved the adjustment of synaptic weight and bias. L–M, Quasi–Newton, Conjugate gradient and Resilient propagation are the most often utilized training algorithms [46–48].

The ANN model receives data from the input layer, processes it in the hidden layers, and further send the results to

Fig. 1 Schematic of a single artificial neuron

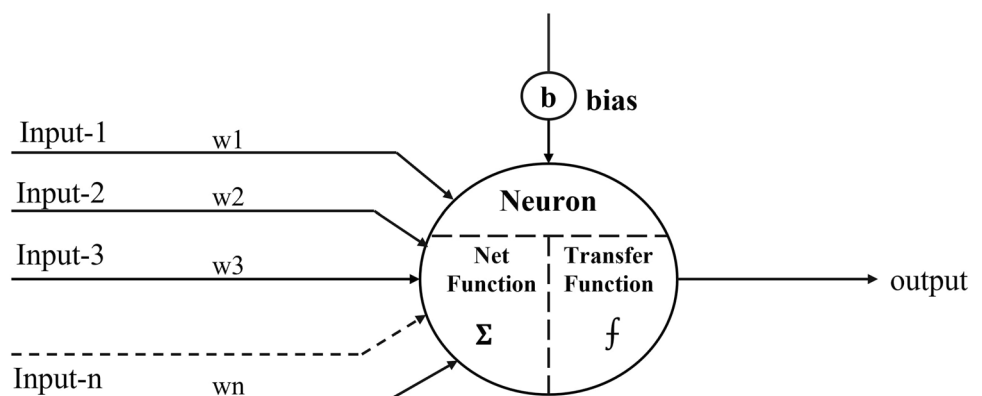
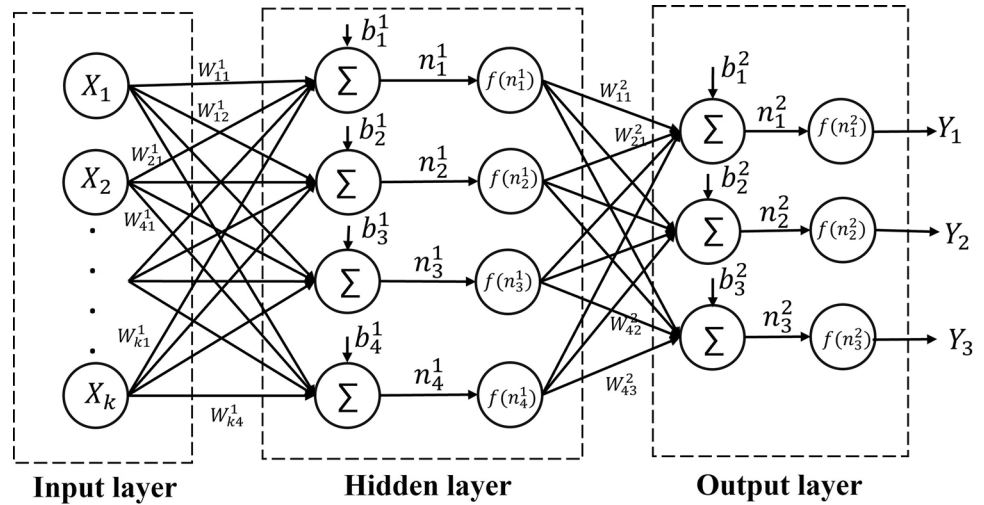


Fig. 2 Architecture of ANN model with single hidden layer



the output layer. At each hidden and output layer, neurons apply the previous layer output to the current layer input. The data in the neurons is changed via a transfer function with weights and bias to compute the results, as follows:

$$Y_j = f\left(\sum_{i=1}^n W_{ji}^n X_i + b_j^n\right) \tag{1}$$

Where, $Y_j = j^{th}$ Neuron output in the hidden layers, $f =$ Activation function, $n =$ Number of layers, $b_j^n =$ Bias of j^{th} neuron, $W_{ji}^n =$ Weight of j^{th} neuron in i^{th} layer, $i =$ Layer, $j =$ Neuron and $X_i =$ Input parameters.

The hidden and the output layers employed sigmoid and purelin activation functions respectively in the ANN architecture. Back-propagation (BP) is a multi-layer network training strategy that employs an iterative gradient descent approach to reduce the mean squared error “E”, which obtained between predicted and desired values:

$$E = \frac{1}{2L} \sum_{j=1}^L [d_j^L - Y_j^L]^2 \tag{2}$$

where $L =$ Number of training patterns, $d =$ Desired output, $Y =$ Predicted output

The weights and biases are modified during the training phase until the predicted error level is attained. The repeated modification of weights and biases is denoted by:

$$W_{ji}^n(k) = W_{ji}^n(k-1) - \alpha \frac{\partial E}{\partial W_{ji}^n} \tag{3}$$

$$b_j^n(k) = b_j^n(k-1) - \alpha \frac{\partial E}{\partial b_j^n} \tag{4}$$

where α and k denote the learning rate and number of iterations for the ANN model, respectively [23].

3 Methodology

Figure 3 depicts the methodology of ANN implementation to predict the flexural strength of ROCGFRP composite laminates. First, three-point bending tests were performed numerically with CZM and experimentally to identify the model input (strain) and output (stress) parameters. Further, the chosen datasets were divided into 70:15:15 for training, validation and test sets respectively. The architecture

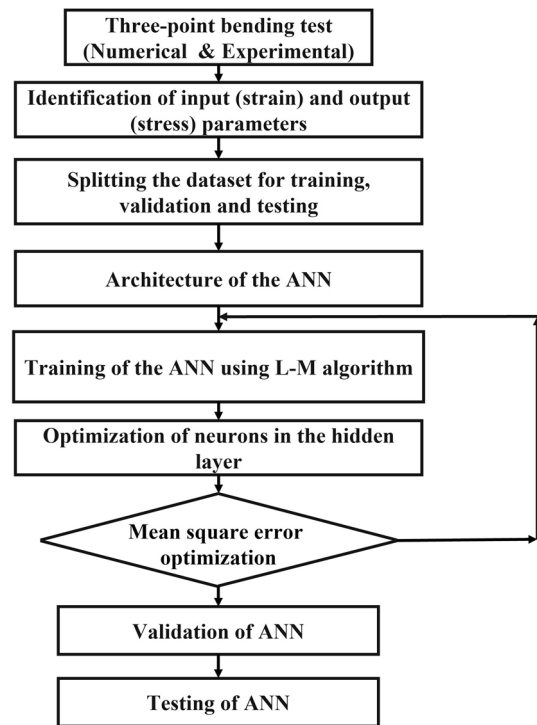


Fig. 3 Methodology for flexural strength prediction of ROCGFRP composite laminate using ANN model

Table 1 Isotropic elasticity property isophthalic polyester resin [11]

Density ($\frac{Kg}{m^3}$)	Poisson's ratio	Young's modulus (MPa)
$\rho = 1120$	$\mu = 0.3$	$E = 3450$

of ANN model is created in MATLAB[®]2021a [49, 50] with the help of code to train and validate the model. The ANN model is trained using the L-M algorithm and number of neuron in the hidden layer is optimized for the least value of RMS error. There after the performance of the model, error histogram and regression are investigated carefully to understand the accuracy of the model. At last, the flexural strength is predicted and compared with the experimental results to check the effectiveness and reliability of ANN model (Table 1).

3.1 Numerical simulation

FEA simulation is carried out in ANSYS workbench 19.2. It consists of following steps: (i) Creation of beam geometry, (ii) definition of material and cohesive zone property, (iii) meshing of geometry, (iv) define cohesive zone for interface delamination and (v) Static structural analysis of beam to compute flexural strength under interface delamination conditions. The basic steps of static analysis FE simulation is demonstrated in Fig. 4.

A rectangular laminate of length 60 cm, width 12 mm and thickness 3.3 mm were modelled in ANSYS workbench ACP (pre). Each ply is made up of randomly oriented chopped glass fiber/resin with thickness of 1.1 mm. Composite laminate consists of three plies and total

Table 3 Cohesive material property [11, 52]

Property	Value
Maximum normal stress (MPa)	25
Normal displacement jumps after debonding (mm)	0.0244
Maximum tangential traction (MPa)	-25
Normal displacement jumps after debonding (mm)	-0.022
Ratio	0.8
Non-dimensional weighted parameter	1

thickness of 3.3 mm. A cohesive zone layer of thickness zero millimetre is defined between the subsequent ply in order to create interface delamination during analysis. Further, three semi-circular strips with 10 mm diameter and 0.5 mm thickness were modelled in ANSYS workbench geometry. The global and local coordinates were appropriately defined to achieve the objective of the experiment. Finally, the rectangular beam and semi-circular strips were imported into static structure for the three-point bending test analysis. The material properties such as isophthalic polyester resin (Refer Table 2) as matrix and randomly oriented chopped glass fiber (Refer Table 3) as reinforced for beam, cohesive material property (See Table 4) for interface delamination and mild steel for semi-circular strip (See Table 4) were chosen as per the research work published by Pankaj & Deepak [11]. The semi-circular strip is placed over the laminate and the frictionless contact is defined between them to meet the requirement of simulation. Figure 5a–c show the top view, front view and isometric view of three-point bend test specimen with the representation of mesh size and boundary conditions, respectively. From Fig. 5c, It can be observed that fixed

Fig. 4 Basic steps of static analysis of FE simulation

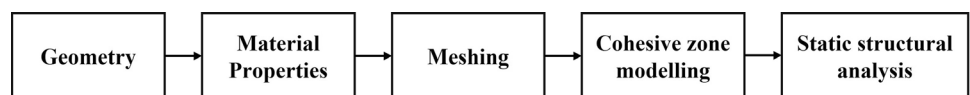


Table 2 Orthotropic property of randomly oriented chopped GFRP [11, 51]

Density ($\frac{Kg}{m^3}$)	Poisson's ratio	Young's modulus (MPa)	Shear Modulus (GPa)	Orthotropic stress limit (MPa)	Orthotropic strain limit
$\rho = 1500$	$\mu_{12} = 0.3$	$E_1 = 6.423$	$G_{12} = 1.727$	$X_t = 1140$	$\epsilon_{xt} = 0.1774$
	$\mu_{23} = 0.4$	$E_2 = 3.430$	$G_{23} = 1.358$	$Y_t = 35$	$\epsilon_{xt} = 0.3309$
	$\mu_{13} = 0.3$	$E_3 = 3.430$	$G_{13} = 1.727$	$Z_t = 35$	$\epsilon_{xt} = 0.3309$
				$X_c = 570$	$\epsilon_{xc} = 0.0887$
				$Y_c = 114$	$\epsilon_{yc} = 0.0332$
				$Z_c = 114$	$\epsilon_{zc} = 0.0332$
				$S_{12} = 72$	$\gamma_{xy} = 0.0416$
				$S_{23} = 52$	$\gamma_{yz} = 0.0382$
				$S_{13} = 72$	$\gamma_{xz} = 0.0416$

Table 4 Structural steel (semi-circular strip) [11]

Property	Value
Density ($\frac{Kg}{m^3}$)	7850
Elastic Modulus (GPa)	200
Poisson's ratio	0.3
Tensile yield strength (MPa)	250
Tensile ultimate strength (MPa)	460

support is applied at the both semi-circular strip placed at the bottom of the beam, A load of 232 N (Calculated using bending strength eq. 5 using experimental result) applied in Y-direction X and Z-direction, respectively at the upper strip. It is assumed that the movement of beam specimen is restricted in X and Z direction.

Meshing is an essential step in the FE simulation process. It affects the accuracy, convergence, and speed of the solution. A four-node quadrilateral element was used to represent the meshing of each rectangular composite layer and the semi-circular strip. Mesh sensitivity analysis was conducted to optimize the computation time. The computation time was decreased by incorporating varied mesh sizes/densities in different parts of the FE model. A fine mesh of size (0.3×0.3) mm was done in the loading zone, and coarse mesh size (0.6×0.6) mm outside the loading zone, where no damage is susceptible to occur. The mesh is said to converge if further mesh refinement results in a negligible change in the solution. From Fig. 6, it is clear that the graph is plotted between equivalent stress, strain energy, and the number of elements (N). After a certain number of elements, the equivalent stress and strain energy values are stable. Therefore, the total number of elements in the rectangular beam and the semi-circular strip is 11,520 as shown in Fig. 6.

3.2 Materials and methods

The randomly oriented chopped GFRP composite laminates of 3 mm thickness were fabricated using a hand lay-up approach. The reinforcing material is used as randomly oriented chopped glass fibre of 459 GSM, and the matrix material is employed as isophthalic polyester resin of RPL-100 to fabricate the composite laminates. The weight ratio of the reinforced material to matrix material is set to be 3:7. Furthermore, the matrix material is mixed with the hardener (methyl ethyl ketone peroxide) at a 10:1 ratio in the beaker. The hardener and isophthalic polyester resin are well stirred with the help of stirrer. Thereafter, a tiny coating of wax is applied to the flat mould surface to erase minor surface flaws like as scratches, stains and oxidation. Followed by, polyvinyl alcohol (PVA) is added to the surface as a chemical release agent to facilitate the removal of the laminate from the mould after manufacture. A layer of randomly oriented chopped glass fiber fabric is laid over the die, followed by a layer of mixture of resin and hardener. This process is continued till the three layers of fabric. Then, the cylindrical roller is used to remove excess amount of resin from the laminate by squeezing. After finishing the hand lay-up, the laminate is cured under atmospheric conditions for atleast 24 hours. After curing, the laminate is removed from the mould and cut to the required dimensions as per the ASTM D790 for the three-point bending test as illustrated in Fig. 7a.

$$\text{Bending Strength}(\sigma_b) = \frac{3FL}{2bt^2} \quad (5)$$

The three point bending test was conducted on four specimens as per the ASTM D790 standard [53]. In this test, a composite laminate with a rectangular cross-section

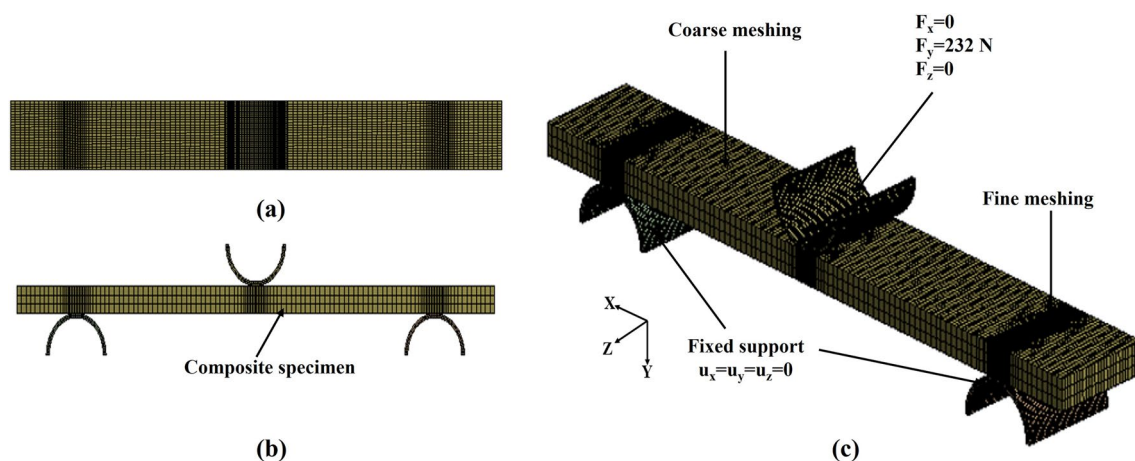


Fig. 5 Schematic representation of geometry, meshing and boundary conditions of laminate **(a)** top view, **(b)** front view and **(c)** isometric view [11]

Fig. 6 Mesh convergence study based on variation of equivalent stress and strain energy with number of elements [11]

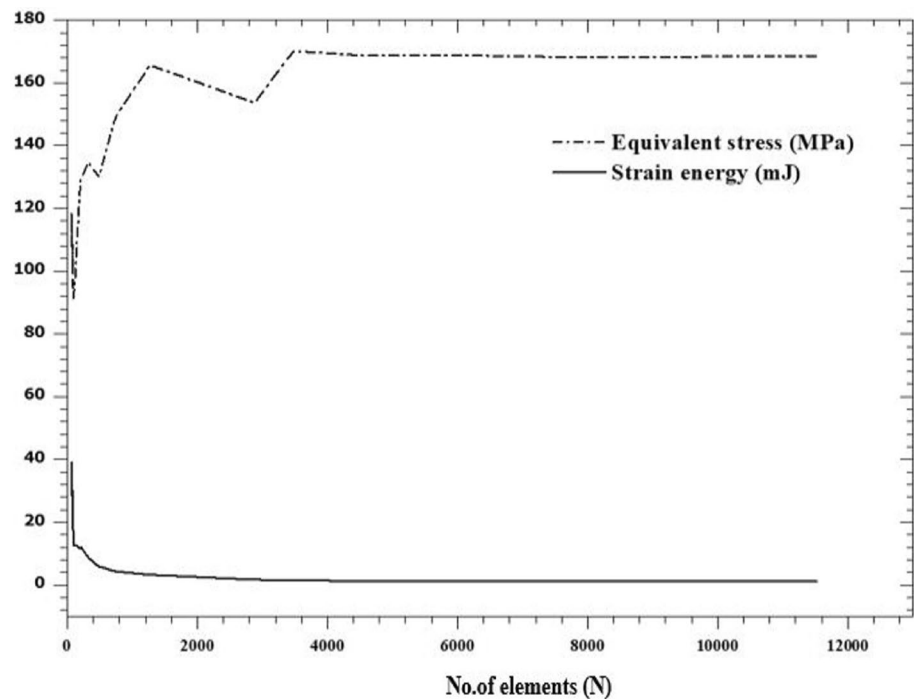
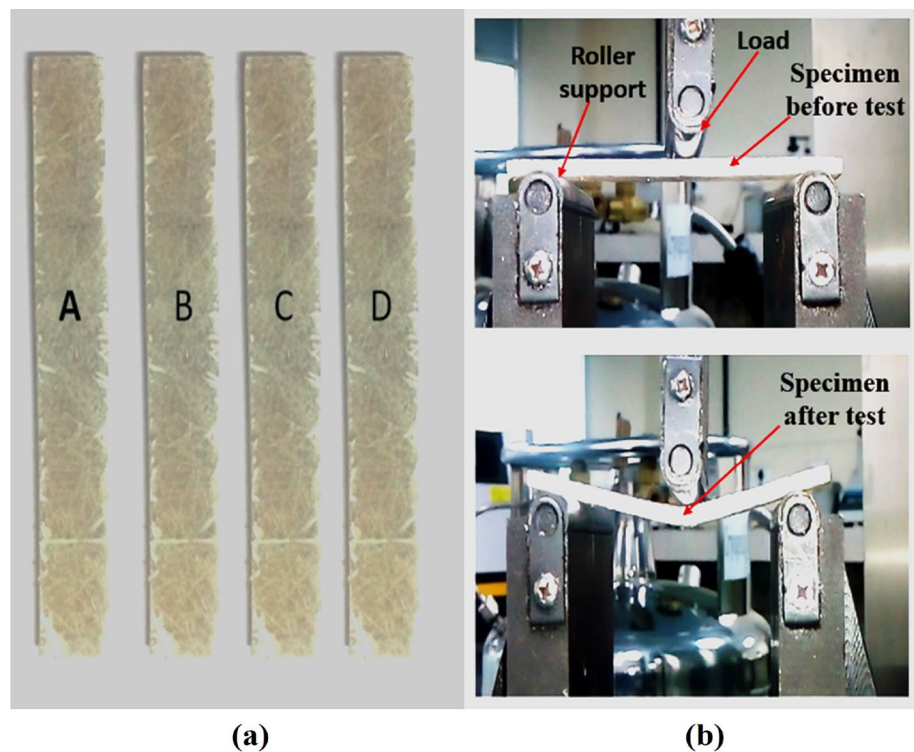


Fig. 7 **a** GFRP test specimen, **b** Three-Point bending test experimental setup [11]



subjected to the simply supported condition and the point load is applied at center of the test specimen. The span between two cylindrical supports is taken in the ratio $L/t = 16:1$ to $32:1$ as per ASTM standard [54]. The bending strength expression is given in Eq. (5). This equation used by the researcher to calculate flexural load for numerical

simulation. Where L = effective length of the test specimen, t = thickness, b = width, and F = applied load. An overhanging length of 10 mm was maintained on both sides of the roller supports, as represented in Fig. 7b. The test specimens final length, width and thickness were considered as 60 mm, 12.25 mm and 3.265 mm, respectively. Blue

Star's 20 kN Electromechanical Universal Testing Machine (Model No: WDW-20) is utilized to conduct the three-point bending test. Figure 7b depicts the UTM test setup and the test specimen before and after the three-point bending test. A constant feed rate of 2 mm/min is maintained during the experimental bending analysis. Followed by the test, a set of data file containing time, load, displacement, stress and strain were obtained. Further, based on the obtained data file, stress-strain curves and ultimate flexural strength are calculated.

4 Results and discussions

The experimental and numerical results of the three-point bending test are briefly explained in this section. Based on the obtained flexural strength from stress-strain curves, ANN models were developed to predict the flexural strength for the ROCGFRP composite laminate.

4.1 Numerical and experimental flexural strength

After completion of FEA simulation, the flexural strength of beam with formation of interface delamination is depicted in Fig. 8. From the figure, it is clearly observed that the interface delamination is occurred between the subsequent ply and corresponding flexural strength found to be 165.31 MPa.

The numerical stress-strain curves for all four specimens are represented in Fig. 9. It is shown that as stress increases, strain grows continually until ultimate strength is reached, i.e., damage initiated in the laminate. Followed by, the stress begins to diminish, and the strain shows no substantial changes due to the subsequent damage propagation of the laminate. The observed average numerical and

experimental flexural strengths are 165.31 MPa and 159.5 MPa, respectively.

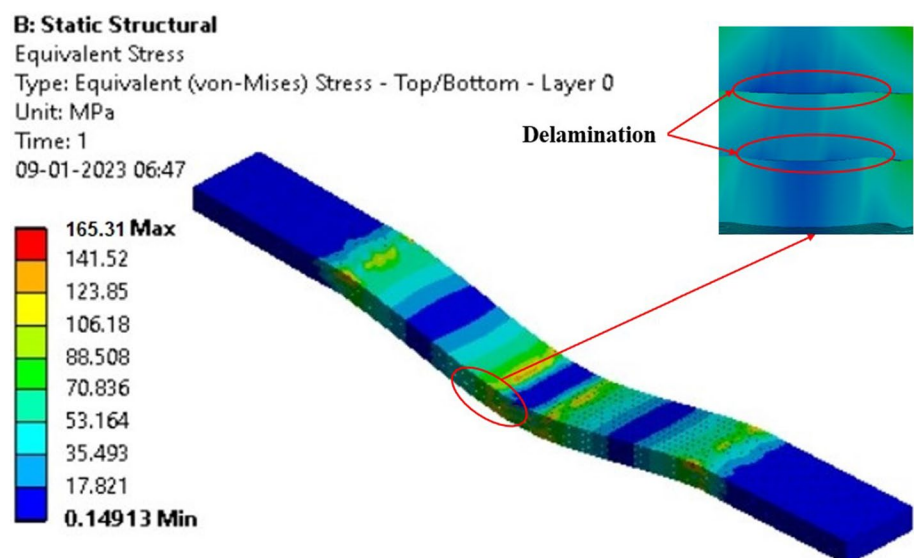
4.2 Testing of artificial neural network (ANN) model

Three-layers ANN called perceptron were modelled using MATLAB[®]2021a. The ANN model was comprised of three layers: the input layer (input neuron), the hidden layer (computational neurons), and the output layer. The three-point bending test was employed to estimate the input and output parameters of the ANN model. The model's input and output were chosen to be strain and stress, respectively. The bending test yielded a total of 7,616 data points, which were analyzed. Furthermore, the data points are divided into 70:15:15 in the proportion of training, testing, and validation respectively. The sigmoid and purelin functions were applied to the hidden and output layers, respectively and the L-M algorithm was used to train the ANN model. The structure of ANN model is shown in Fig. 10.

4.2.1 Optimization of neurons in hidden layer

The hidden layer in the ANN model is the layer between the input and output layers. The hidden layer's function is to perform the computation, and it is used to solve the non-linear problems. As a result, defining the number of hidden layers and neurons in each hidden layer is critical. The number of hidden layers cannot be determined deterministically. It can be decided by the hit and trial method only. In general, zero hidden layers are chosen for linear problems, and one or more hidden layers are chosen for complex problems. As a result, one hidden layer was chosen for ANN model. The hidden layer's number of neurons was optimized by plotting a graph between the number of neurons and root mean

Fig. 8 Schematic representation of numerical flexural strength with delamination in the composite laminate



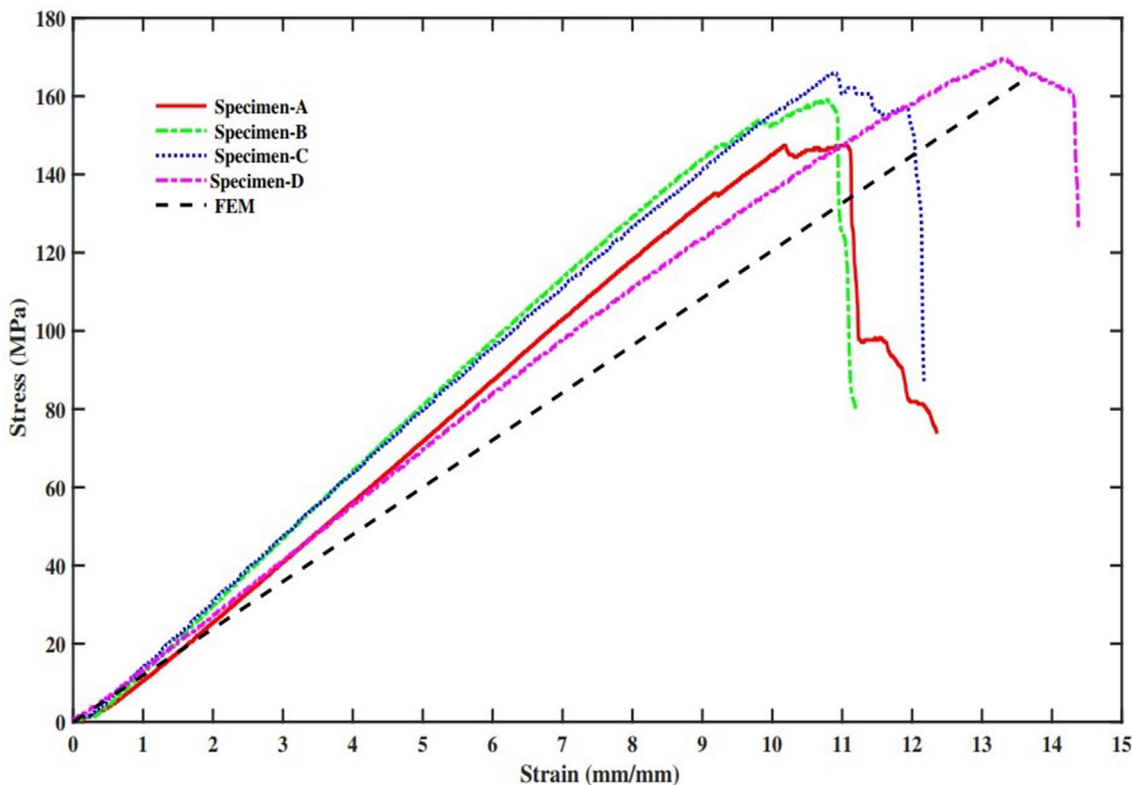


Fig. 9 Stress-Strain curves of ROCGFRP composite laminates

Fig. 10 Structure of artificial neural network (ANN) model

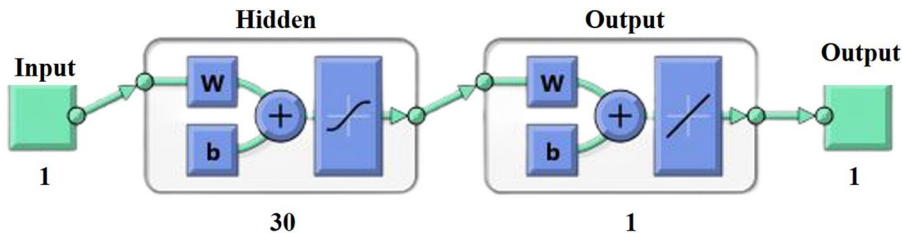
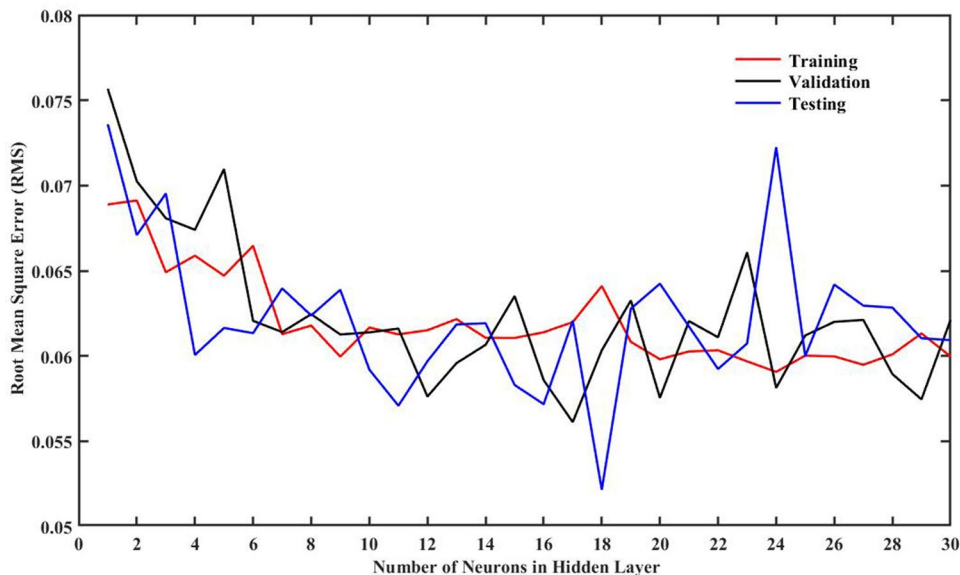


Fig. 11 Selection of optimum number of neurons in the hidden layer



square (RMS), as shown in Fig. 11. According to Fig. 11, the optimal number of neurons in the hidden layer can be chosen as 18. At this point, the RMS error value for the validation set is negligible, while the training and testing sets are substantial quantities.

4.2.2 Performance of the model

The present ANN model is trained using the L-M algorithm, and the performance of the model's is plotted in Fig. 12. The training process of the current model is completed at fifty-nine epochs as shown in Fig. 12, but it does not give the minimum mean square error. Thus, the algorithm selects fifty-three as the optimum number of epochs, corresponding to the most negligible MSE value, i.e., 0.0041189. Figure 13 represents the training state of the model. This gradient is $1.0875e-5$, learning rate for the L-M algorithm (μ) is $1e-6$, corresponding to fifty-nine epochs. Further, it can be seen that after six validation fails, the training process is stopped. The obtained RMS values are 0.0619, 0.0610, and 0.617 for the training, validation and test sets, respectively.

4.2.3 Error histogram

The error histogram as shown in Fig. 14, which depicts network performances, training, validation and test data were represented by the blue, green and red bars, respectively. The error histogram is identified by the outliers, which means the data points that have a much inferior fit than the rest of the data. [49]. The x-axis represents the vertical bars on

the graph called bins. The error varies between -0.3509 and 0.2403. The error range is divided into 20 small bins and the calculated width for each bin is 0.02956. Each vertical bar represented the number of samples from data sheets and was represented on the y-axis. The zero error line denotes the maximum level of precision. The majority of the datasets are close to the zero error line. As a result, the trained model can predict the future cases successfully.

4.2.4 Regression analysis

From Fig. 15a–c, the regression values computed by ANN models are 0.98031, 0.97647 and 0.97717 for training, validation and testing, respectively, while Fig. 15d represents combined regression value of 0.97927 for training, validation and testing. The data sets for the training, validation and test components are fitted along the regression line. It demonstrated that there is a strong relationship between analysis and desired outcomes.

4.2.5 Predicted flexural strength

The combined number of experimental and numerical data points and corresponding flexural strength value is plotted on X and Y axis, respectively as shown in Fig. 16. The predicted value of flexural strength computed by the ANN algorithm is also plotted corresponding to the given data points. It is observed that predicted flexural strength values are almost coincide with the experimental values and the RMS error value is 0.0604 i.e, 6.04 percentage, which

Fig. 12 Number of epochs

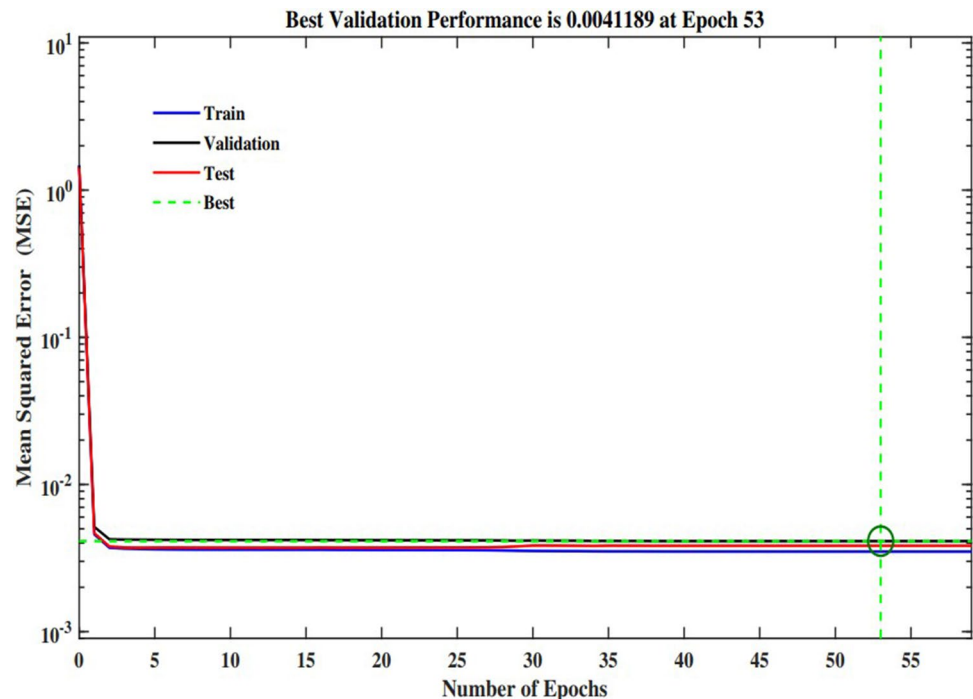


Fig. 13 State of the model after training

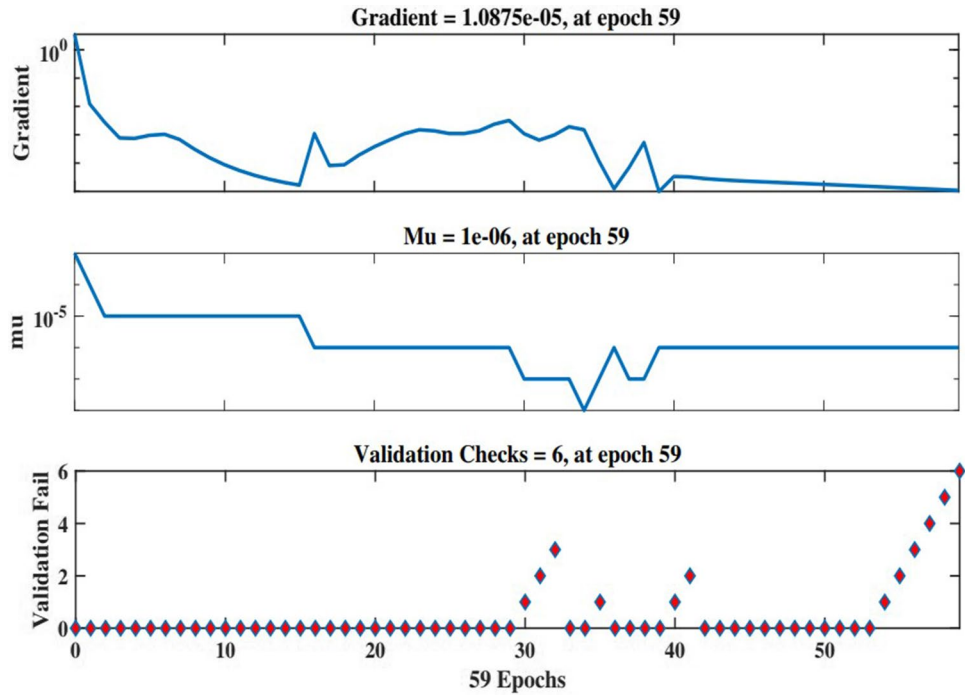
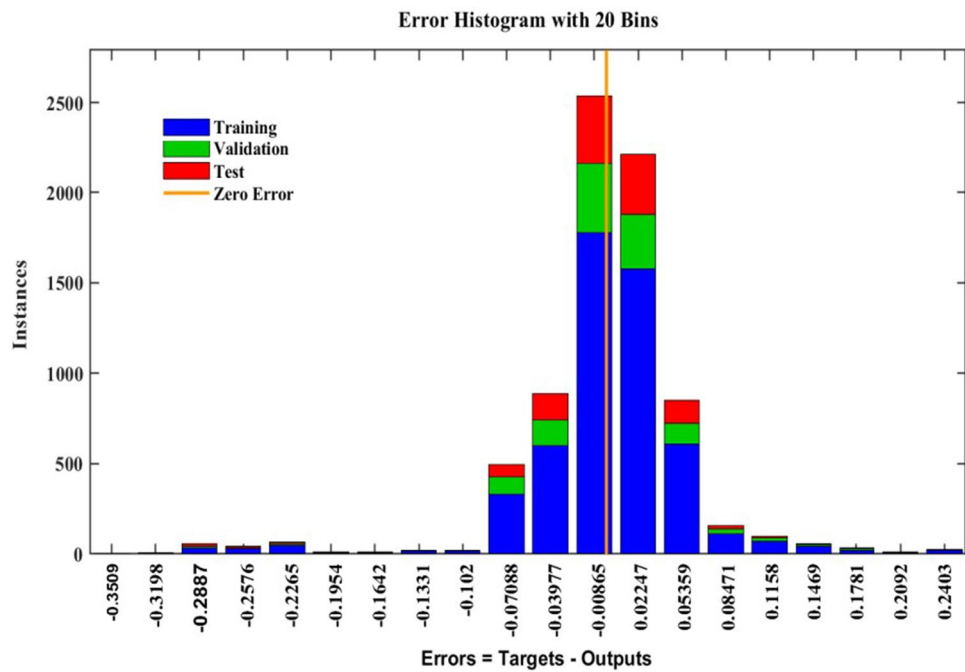


Fig. 14 Error histogram with 20 Bins



seems to be considerably low. This justifies that ANN model is highly efficient and can predict the flexural strength of randomly oriented GFRP accurately.

5 Conclusions

In this study, the flexural strength of ROCGFRP composite laminates were predicted using ANN model. CZM was implemented in FE simulation to compute the numerical flexural strength under interface-delaminated conditions. Three-point bending test was conducted on the four

Fig. 15 Regression analysis of (a) Training, b Validation, c Test and d Combined results

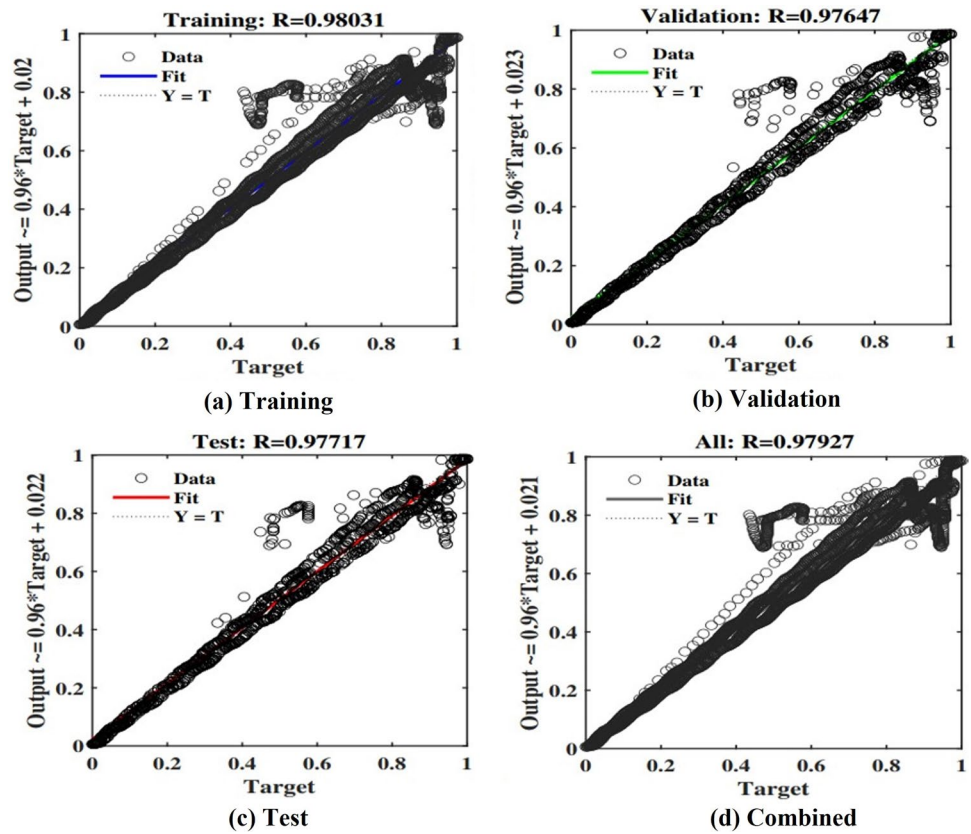
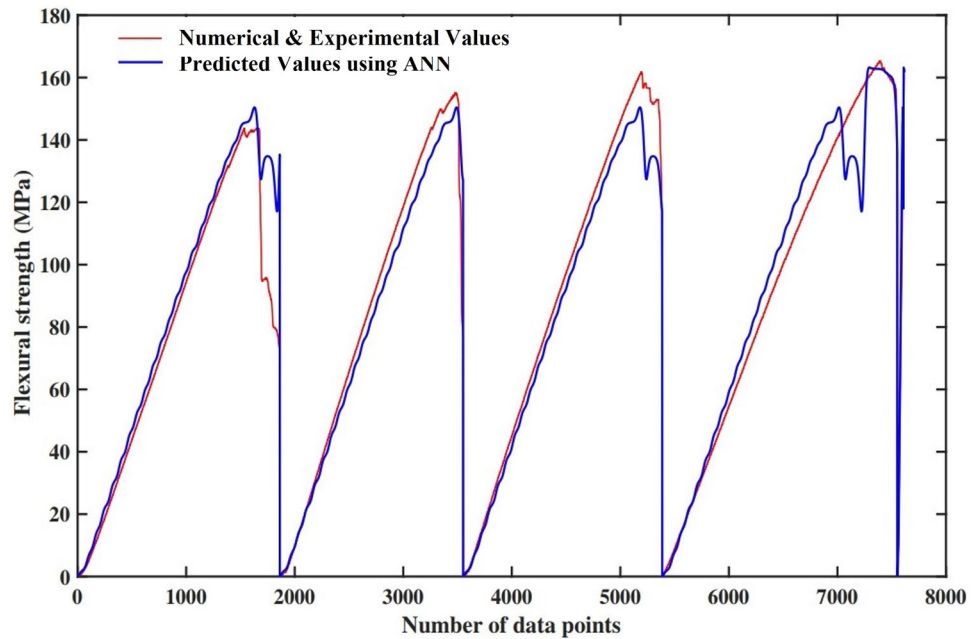


Fig. 16 Comparison between predicted and experimental flexural strengths



specimens to investigate the flexural strength and ultimate load-bearing capacity of the materials. Further, experimental and numerical results were combined for ANN analysis. The computed flexural strength numerically and experimentally were found to be 165.31 and 159.5 Mpa,

respectively. The structure of ANN model was created as follows: strain was chosen as input, stress as output, L-M as training algorithm, sigmoid as activation function for hidden layer and purelin for out layer, respectively. The complete dataset is divided into training, validation and

testing in the proportion of 70:15:15, respectively. The optimal number of neurons in the hidden layer was determined to be 18, which corresponded to the lowest RMS values. The training, validation, and testing regression coefficients were 0.98031, 0.977647 and 0.97717, respectively. The best validation performance was observed at 53 epochs. The training, validation, and test root mean square values were 0.0619, 0.0610, and 0.617, respectively. Finally, the predicted values of flexural strength computed by the ANN were found to be highly consistent with the experimental values.

References

- Jones RM (2018) *Mechanics of composite materials*. CRC Press, London
- BK Chaurasia, D Kumar, and MK Paswan (2022) Experimental studies of failure in l-shaped carbon fiber-reinforced polymer composite under pullout and four-point bending. *J Inst Eng (India): Ser D*, pp. 1–11
- Elkazaz E, Crosby W, Ollick A, Elhadary M (2020) Effect of fiber volume fraction on the mechanical properties of randomly oriented glass fiber reinforced polyurethane elastomer with cross-head speeds. *Alex Eng J* 59(1):209–216
- Peret T, Clement A, Freour S, Jacquemin F (2017) Effect of mechanical states on water diffusion based on the free volume theory: Numerical study of polymers and laminates used in marine application. *Compos B Eng* 118:54–66
- Kootsookos A, Mouritz AP (2004) Seawater durability of glass-and carbon-polymer composites. *Compos Sci Technol* 64(10–11):1503–1511
- Lau K-T, Hung P-Y, Zhu M-H, Hui D (2018) Properties of natural fibre composites for structural engineering applications. *Compos B Eng* 136:222–233
- Prakash C, Sekar KV (2018) 3d finite element analysis of slot milling of unidirectional glass fiber reinforced polymer composites. *J Braz Soc Mech Sci Eng* 40(6):1–13
- Shenoi R, Dodkins A (2000) Design of ships and marine structures made from frp composite materials. *Comprehen Compos Mater* 6:429–449
- Park S-J, Seo M-K (2011) *Interface science and composites*, vol 18. Academic Press, London
- Seghi RR, Sorensen JA (1995) Relative flexural strength of six new ceramic materials. *Int J Prosthodont* 8:239–239
- P Chaupal and D Kumar (2022) Progressive damage analysis of random oriented chopped glass fiber-reinforced laminate under three-point bending test. *J Inst Eng (India) Ser D* pp. 1–14, 2022
- Ramnath BV, Elanchezhan C, Jeykrishnan J, Ragavendar R, Rakesh P, Dhamodar JS, Danasekar A (2018) Implementation of reverse engineering for crankshaft manufacturing industry. *Mater Today Proc* 5(1):994–999
- Hartsuijker C, Welleman J (2007) Shear forces and shear stresses due to bending. *Engineering mechanics: stresses, strains, displacements*, pp 271–409
- Chaudhary S, Singh K, Venugopal R (2018) Experimental and numerical analysis of flexural test of unfilled glass fiber reinforced polymer composite laminate. *Mater Today Proc* 5(1):184–192
- G. Rathnakar and H. Shivanan (2013) Experimental evaluation of strength and stiffness of fibre reinforced composites under flexural loading. *Int J Eng Innov Technol (IJEIT)* vol. 2, no. 7
- Galhano GÁ, Valandro LF, De Melo RM, Scotti R, Bottino MA (2005) Evaluation of the flexural strength of carbon fiber-, quartz fiber-, and glass fiber-based posts. *J Endodont* 31(3):209–211
- El-Wazery M, El-Elamy M, Zoalfakar S et al (2017) Mechanical properties of glass fiber reinforced polyester composites. *Int J Appl Sci Eng* 14(3):121–131
- Cavalcanti D, Banea M, Neto J, Lima R, Da Silva L, Carbas R (2019) Mechanical characterization of intralaminar natural fibre-reinforced hybrid composites. *Compos B Eng* 175:107149
- Dong C (2020) Flexural properties of symmetric carbon and glass fibre reinforced hybrid composite laminates. *Compos Part C Open Access* 3:100047
- Jiang X, Song J, Qiang X, Kolstein H, Bijlaard F (2016) Moisture absorption/desorption effects on flexural property of glass-fiber-reinforced polyester laminates: Three-point bending test and coupled hygro-mechanical finite element analysis. *Polymers* 8(8):290
- Cheng P, Peng Y, Wang K, Wang Y-Q (2021) Mechanical performance and damage behavior of delaminated composite laminates subject to different modes of loading. *J Braz Soc Mech Sci Eng* 43(10):1–10
- Wang S-C (2003) *Interdisciplinary computing in Java programming*, vol 743. Springer, Cham
- Jiang Z, Gyurova L, Zhang Z, Friedrich K, Schlarb AK (2008) Neural network based prediction on mechanical and wear properties of short fibers reinforced polyamide composites. *Mater Des* 29(3):628–637
- Chiachio M, Chiachio J, Rus G (2012) Reliability in composites-a selective review and survey of current development. *Compos B Eng* 43(3):902–913
- Ranković V, Grujović N, Divac D, Milivojević N (2014) Development of support vector regression identification model for prediction of dam structural behaviour. *Struct Saf* 48:33–39
- H Tanyildizi (2018) Prediction of the strength properties of carbon fiber-reinforced lightweight concrete exposed to the high temperature using artificial neural network and support vector machine. *Adv Civ Eng*
- Zhang Z, Friedrich K (2003) Artificial neural networks applied to polymer composites: a review. *Compos Sci Technol* 63(14):2029–2044
- Mentges N, Dashtbozorg B, Mirkhalaf S (2021) A micromechanics-based artificial neural networks model for elastic properties of short fiber composites. *Compos Part B Eng* 213:108736
- Hassan AKF, Mohammed LS, Abdulsamad HJ (2018) Experimental and artificial neural network ann investigation of bending fatigue behavior of glass fiber/polyester composite shafts. *J Braz Soc Mech Sci Eng* 40(4):1–10
- Vineela MG, Dave A, Chaganti PK (2018) Artificial neural network based prediction of tensile strength of hybrid composites. *Mater Today Proc* 5(9):19908–19915
- Stephen C, Thekkuden DT, Mourad A-HI, Shivamurthy B, Selvam R, Behara SR (2022) Prediction of impact performance of fiber reinforced polymer composites using finite element analysis and artificial neural network. *J Braz Soc Mech Sci Eng* 44(9):1–11
- P Chopra, RK Sharma, and M Kumar (2016) Prediction of compressive strength of concrete using artificial neural network and genetic programming. *Adv Mater Sci Eng*
- Koker R, Altinkok N, Demir A (2007) Neural network based prediction of mechanical properties of particulate reinforced metal matrix composites using various training algorithms. *Mater Des* 28(2):616–627
- Shmueli G, Bruce PC, Yahav I, Patel NR, Lichtendahl KC (2017) *Data mining for business analytics: concepts, techniques, and applications in R*. Wiley, London
- Pazhamannil RV, Govindan P, Sooraj P (2021) Prediction of the tensile strength of polylactic acid fused deposition models

- using artificial neural network technique. *Mater Today Proc* 46:9187–9193
36. Kumar CS, Arumugam V, Sengottuvelusamy R, Srinivasan S, Dhakal H (2017) Failure strength prediction of glass/epoxy composite laminates from acoustic emission parameters using artificial neural network. *Appl Acoust* 115:32–41
 37. Lucon PA, Donovan RP (2007) An artificial neural network approach to multiphase continua constitutive modeling. *Compos B Eng* 38(7–8):817–823
 38. Ootao Y, Tanigawa Y, Nakamura T (1999) Optimization of material composition of fgm hollow circular cylinder under thermal loading: a neural network approach. *Compos B Eng* 30(4):415–422
 39. Livingstone DJ (2008) *Artificial neural networks: methods and applications*. Springer, Cham
 40. Hossain MS, Ong ZC, Ismail Z, Noroozi S, Khoo SY (2017) Artificial neural networks for vibration based inverse parametric identifications: a review. *Appl Soft Comput* 52:203–219
 41. Carden EP, Fanning P (2004) Vibration based condition monitoring: a review. *Struct Health Monit* 3(4):355–377
 42. Worden K, Dulieu-Barton JM (2004) An overview of intelligent fault detection in systems and structures. *Struct Health Monit* 3(1):85–98
 43. Hakim S, Razak HA (2014) Modal parameters based structural damage detection using artificial neural networks-a review. *Smart Struct Syst* 14(2):159–189
 44. Antsaklis PJ et al (1990) Neural networks for control systems. *IEEE Trans Neural Networks* 1(2):242–244
 45. Getahun MA, Shitote SM, Gariy ZCA (2018) Artificial neural network based modelling approach for strength prediction of concrete incorporating agricultural and construction wastes. *Constr Build Mater* 190:517–525
 46. Hagan MT, Menhaj MB (1994) Training feedforward networks with the Marquardt algorithm. *IEEE Trans Neural Netw* 5(6):989–993
 47. Zakaria Z, Isa NAM, Suandi SA (2010) A study on neural network training algorithm for multiface detection in static images. *Int J Comput Inf Eng* 4(2):345–348
 48. Chng E, Chen S, Mulgrew B (1996) Gradient radial basis function networks for nonlinear and nonstationary time series prediction. *IEEE Trans Neural Netw* 7(1):190–194
 49. MH Beale, MT Hagan, and HB Demuth (1992) *Neural network toolbox user's guide*. The MathWorks Inc, vol. 103
 50. Beale MH, Hagan MT, Demuth HB (2010) *Neural network toolbox. User's Guide*, MathWorks 2:77–81
 51. Mousavi MV, Khoramishad H (2019) The effect of hybridization on high-velocity impact response of carbon fiber-reinforced polymer composites using finite element modeling, Taguchi method and artificial neural network. *Aerospace Sci Technol* 94:105393
 52. Waseem M, Kumar K (2014) Finite element modelling for delamination analysis of double cantilever beam specimen. *Int J Mech Eng* 1(5):27–34
 53. I ASTM (2007) *Standard test methods for flexural properties of unreinforced and reinforced plastics and electrical insulating materials*. ASTM D790–07
 54. Harper L, Ahmed I, Felfel R, Qian C (2012) Finite element modelling of the flexural performance of resorbable phosphate glass fibre reinforced pla composite bone plates. *J Mech Behav Biomed Mater* 15:13–23

Publisher's Note Springer Nature remains neutral with regard to jurisdictional claims in published maps and institutional affiliations.

Springer Nature or its licensor (e.g. a society or other partner) holds exclusive rights to this article under a publishing agreement with the author(s) or other rightsholder(s); author self-archiving of the accepted manuscript version of this article is solely governed by the terms of such publishing agreement and applicable law.